Proceedings of the
44th IEEE Conference on Decision and Control, and
the European Control Conference 2005
Seville, Spain, December 12-15, 2005

Experimental Validation of Nonlinear Dynamic Models for Single-Link Very Flexible Arms

Ismael Payo, Francisco Ramos, O. Daniel Cortázar and Vicente Feliu*

Abstract— **This paper proposes some new nonlinear dynamic models for single-link flexible manipulators that experience large deflections. These models are developed under the assumption of a very lightweight arm with all its mass concentrated at the tip. Two models are proposed that are validated experimentally. The first of them is the typical linear model. The second one is a new nonlinear model that exhibits the advantages of being very simple while being very accurate too. Compared with the previously defined models, which are based on finite elements numerical techniques, our models are described by nonlinear ordinary differential equations that are well suited for analysis and design of closed loop control systems for tip positioning.**

Index Terms— **Nonlinear dynamics; Flexible arms.**

I. Introduction

In the last two decades, flexible robots have become a research area of increasing interest in engineering. Because of high performance requirements in robotics (high speed operation, minimization of collision effects) and space applications (very large lightweight robots), controlling the structural flexibility in such way that oscillations at the tip are removed is an active field of research (see [1] for a recent survey on this).

Different dynamic models have been proposed for analysis and control of these robots: the basic spring-mass discrete model ([2], e.g.), lumped masses models ([3], e.g.) linear Euler-Bernoulli PDE ([4], e.g.), generalized Newton-Euler algorithms ([5], e.g.), Lagrangian equations ([6], e.g.), associated to a Rayleigh-Ritz elastic field decomposition method, finite element decomposition ([7], [8], e.g.), or modal decomposition. All these models are accurate under the assumption of small elastic displacements.

Some work has also been devoted to model large elastic displacements. Based on the Euler-Bernouilli equation, numerical algorithms have been proposed to estimate the curvature and tip deflection of an static elastic beam. These methods rely on the solution of complicated integral equations by numerical methods [9], [10], numerical solution of nonlinear differential equations ([11] for fixed cross sections and nonlinear elastic materials and [12] for variable cross section), or the use of sensors (strain gauges) that measure the curvatures at certain points of the beam followed by a polynomial interpolation [13]. Finally, some work has also been carried out on non linear dynamics of multibody mechanical systems composed of Euler Bernouilli beams ([14], [15] e.g.).

Some of the modeling techniques before mentioned give precise descriptions of the geometrical nonlinear dynamics of the flexible beam, even in the 3D space. These models are based on numerical approximations of differential or integral equations that have to be solved at every considered time, or they are represented by means of complicated analytical differential equations. They are well suited for numerical simulations or for calculating command profiles (usually motor torques) to be applied in an open loop fashion to the arm in order to follow a desired tip trajectory. But these models can hardly be applied to analyze and design nonlinear closed loop control systems for these arms. At most, linearized models of local validity around the desired trajectory can be derived from the before models, which may lead to local linear controllers that need to be updated in real time in function of the state of the arm.

We are interested in simple nonlinear dynamic models, that capture the most important dynamics of the arm while remaining useful for the design of arm tip position nonlinear controllers. Then in this paper we propose an approach completely different from the previous ones, which is based on identifying the arm dynamics from experimental data. This experimental data will show us which nonlinear terms are relevant in the dynamic behavior of the arm.

Most of the research on control of flexible manipulators deals with the single-link case arm (again we refer to [1] e.g.). Moreover we are interested in studying the case of large deflections which are caused by motions of very flexible arms. Often this large flexibility appears in beams of very small cross section, which is consequence of the engineers desire of designing an arm as lightweight as possible. Then this paper studies the dynamics of a single-link very slender flexible arm built of composite materials, under the assumption that all its mass is concentrated at the tip (only payload mass is significant). This assumption often describes accurately the characteristics of large arms with small cross section.

This paper is organized as follows. Section II states the general nomenclature and the kinematic equations of the Euler-Bernouilli beam. A complete dynamic model including motor dynamics is described in Section III. The simplified dynamic models that we propose for validation are also presented in this Section. Section IV describes the experimental

This work has been supported by the Consejería de Ciencia y Tecnología of the Junta de Comunidades de Castilla-La Mancha (GR-02-012), the CICYT spanish government program (DPI2003-03326) and the European Social Fund

All authors are with E.T.S. Ingenieros Industriales, University of Castilla-La Mancha, Ingeniería Eléctrica, Electrónica y Automática, Campus Universitario s/n, 13071 Ciudad Real, Spain

*Corresponding author: Vicente.Feliu@uclm.es

0-7803-9568-9/05/$20.00 ©2005 IEEE

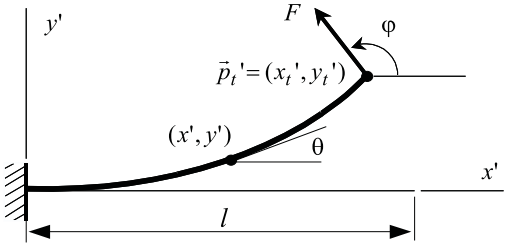

Fig. 1. Large deflection of a one side clamped beam

setup, the procedure to identify of the parameters of our model, and the validation of it. Finally, some conclusions are presented in Section V.

II. Kinematics of the Euler-Bernoulli beam

A very flexible arm exhibits a nonlinear behaviour when it is under the effects of large forces [16]. We assume that our composite material remains linearly elastic and there is not a change of status. Then, nonlinear behavior is due to geometric nonlinearities. Under this assumption, the equation of Euler-Bernoulli for large deflections is:

$$\frac{d\theta}{ds} = \frac{\frac{d^2y'}{dx'^2}}{(1+(\frac{dy'}{dx'})^2)^{\frac{3}{2}}} = \frac{M}{EI} \tag{1}$$

where θ is the orientation of the beam at point s, and s is the arc length over the beam, x' and y' are the coordinates of a point of the beam expressed in a Cartesian frame according to Fig. 1, M is the bending moment on any section of the beam and EI is the stiffness of the bar. For small deflections s is equal to x', and the rotation angle θ can be approximated by dy'/dx' yielding that $d\theta/ds$ can be approximated by d^2y'/dx'^2. So, equation of Euler-Bernoulli for small deflections is:

$$EI(\frac{d^2y'}{dx'^2}) = M \tag{2}$$

However, for large deflections these simplifications are not valid and it is necessary to use the above equation (1). The solution of this equation can be obtained by calculating some elliptic integrals, which can be evaluated using numerical methods [9], [10]. Equation (1) does not have an analytical solution.

Consider the Fig. 1, where a force $\vec{F}$ is applied at the tip of the beam. Let us denote the magnitude of this force as F and its orientation as φ. Then, the static (kinematic) equation of the beam is obtained from[17]:

$$\frac{d^2\theta}{ds^2} = \frac{F}{EI}sin(\theta-\varphi) \quad 0 \le s \le l \tag{3}$$

being l the beam length.

The solution of this differential equation is based on an elliptical integral and its numerical solution leads to a generic expression, (particularized at the tip position), of the form:

$$\vec{F} = \vec{\Phi}\,(\vec{p}_t\,', l, EI) = \vec{\Phi}\,(\rho'_t, \theta'_t, l, EI) \tag{4}$$

where ρ'_t and θ'_t are the polar coordinates of the tip position in the frame (x', y').

Defining a normalized force $F_n = \dfrac{Fl^2}{EI}$ and a normalized arc length $s_n = \dfrac{s}{l}$ and substituting in (3), it yields:

$$\frac{d^2\theta}{ds_n^2} = F_n sin\,(\theta-\varphi) \quad 0 \le s_n \le l \tag{5}$$

which is a normalized equation independent of the geometric dimensions of the bar and its elasticity coefficient E, which gives now a solution of the form:

$$\vec{F}_n = \vec{\Phi}_n\,(\rho'_{tn}, \theta'_t) \tag{6}$$

being $\rho'_{tn} = \dfrac{\rho'_t}{l}$.

III. Dynamical models

This Section describes the general dynamic model of our system and, subsequently, presents a linear and a non linear simplified models which will be used for approximating the experimental results in Section IV.

A. General model

Let us consider the model of Fig. 2, where the frame (x, y) is fixed and frame (x', y') is aligned with the beam base (it rotates with motor angle). Assuming that all the mass is concentrated at the tip, so we assume a zero mass link as well, and that it can be considered as a point mass (with null inertia and, consequently, no torques are produced at the tip), the dynamic model for a very flexible nonlinear arm can be expressed by the following general equation:

$$-\vec{\Phi}(\rho_t(t), \theta_t(t)-\theta_m(t), l, EI) = m\frac{d^2\vec{p}_t(t)}{dt^2} \tag{7}$$

obtained from (4) by simply taking into account that $\rho'_t = \rho_t$, $\theta'_t = \theta_t - \theta_m$ and $\vec{F} = -m\dfrac{d^2\vec{p}_t}{dt^2}$, and being ρ_t the tip radius, θ_t and θ_m the tip and the motor angles respectively, m the tip mass and $\vec{p}_t$ the tip position, all of them expressed in the absolute cartesian frame (x, y) of Fig. 2. If we expand the acceleration in polar coordinates, the obtained expressions are

$$\ddot{p}_{tx} = \ddot{\rho}_t\cos\theta_t - 2\dot{\rho}_t\sin\theta_t\dot{\theta}_t - \rho_t\cos\theta_t\dot{\theta}_t^2 - \rho_t\sin\theta_t\ddot{\theta}_t \tag{8a}$$

$$\ddot{p}_{ty} = \ddot{\rho}_t\sin\theta_t + 2\dot{\rho}_t\cos\theta_t\dot{\theta}_t - \rho_t\sin\theta_t\dot{\theta}_t^2 + \rho_t\cos\theta_t\ddot{\theta}_t \tag{8b}$$

By substituting these equations in (7) we obtain the final expression of this model.

Equation (7) allows a subsequent normalization making $t_n = t/\sqrt{m}$. Then

$$-\vec{\Phi}_n(\rho_{tn}, \theta_t-\theta_m) = \frac{d^2\vec{p}_{tn}}{dt_n^2} \tag{9}$$

where $\vec{p}_{tn} = \vec{p}_t/l$.

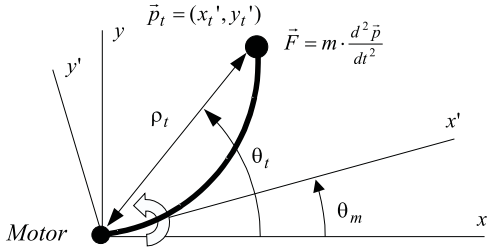

Fig. 2. Dynamic deflection model

Model (7), or (9), has to be completed with the equation of motor dynamics. This is a well-known equation:

$$\Gamma_m = Ki = Jn^2 \frac{d^2\theta_m}{dt^2} + \nu n^2 \frac{d\theta_m}{dt} + \Gamma_c \tag{10}$$

where Γ_m is the torque produced by the motor, K is the electromechanical constant of the motor, i is the current supplied to the motor, n is the reduction relation of the gear, and J and ν are the inertia and the viscous friction of the motor-gear, respectively. Variable Γ_c is the coupling torque between the motor and the tip, which is of the form:

$$\Gamma_c = -\vec{p}_t \times \vec{\Phi}\left(\rho_t, \theta_t - \theta_m, l, EI\right) = -F\rho_t \sin\left(\varphi - \theta_t\right) \tag{11}$$

where $\times$ is vectorial product.

Next we propose several simplifications of the above model (7). First we consider the well known linear approximation model. Then we present our non linear proposed model.

B. Linear model

The classical linear model is established under the assumptions that $\rho_t = l \ \forall t$, and the stiffness function (4) is

$$\Phi_l = \frac{3EI}{l}\theta_t' \tag{12}$$

As $\rho_t = l$, polar coordinates are used to represent these dynamics, only the angle is variable, and $\vec{\Phi}_l$ is a scalar function given by (12).

By denoting $\omega^2 = 3EI/ml^3$ in (7), and taking into account that $\rho_t = l$, operating expressions (7) and (8) yields to

$$\ddot{\theta}_t + \xi_l\dot{\theta}_t + \omega^2\left(\theta_t - \theta_m\right) = 0 \tag{13}$$

where a friction term $\xi_l\dot{\theta}_t$ has been added in order to consider friction at the tip mass and internal energy dissipation in the beam.

C. Nonlinear model

As long as our arm exhibits large deformations, the tip radius can not be considered constant, and the linear deflection model (12) no longer holds true. Next we propose a new nonlinear model that approximates these effects.

Material	Length (mm)	Diameter (mm)
Fibreglass	1000	3
Cross section inertia (m^4)	**Young's modulus (Pa)**	**Density (kg/m^3)**
$3.98 \cdot 10^{-12}$	$31.65 \cdot 10^9$	1761.7

TABLE I
DATA OF THE FLEXIBLE BEAM

1) Nonlinear model for the tip angle: We assume here the equation typically used to model the stiffness of nonlinear springs:

$$\Phi_{nl} = \hat{\alpha}\theta_t' + \hat{\beta}\theta_t'^3 \tag{14}$$

In this case, the resulting dynamic equation of the beam is:

$$\ddot{\theta}_t + \xi_{nl}\dot{\theta}_t + \alpha\left(\theta_t - \theta_m\right) + \beta\left(\theta_t - \theta_m\right)^3 = 0 \tag{15}$$

where $\alpha = \hat{\alpha}/ml$ and $\beta = \hat{\beta}/ml$.

2) Nonlinear model for tip radius: We have carried out extensive numerical simulations of (5) for large values of $\vec{F}$. They show that a good approximation of the tip radius variation is given by the function:

$$\rho_t = l\cos\left(\gamma\left(\theta_t - \theta_m\right)\right) \tag{16}$$

where γ is a parameter to be adjusted.

This model implies that changes in ρ_t basically depend on the component of the force $\vec{F}$ which is tangential to the arc motion, (perpendicular to $\vec{p}_t$), being of second order the effects of the radial component of $\vec{F}$ (component in the direction of $\vec{p}_t$).

IV. EXPERIMENTAL VALIDATION

This Section is devoted to experimentally validate the previous models. Model parameters are fitted to experimental data, and their validity is checked then by comparing such experimental data with the simulated responses of these models.

A. Experimental setup description

Fig. 3 shows a picture of the used experimental platform. One end (base), of the flexible bar is attached to an Harmonic Drive mini servo DC motor RH-8D-6006-E036AL-SP(N) which has a reduction relation $n = 50$. At the other end (tip), there is a disc mass that can freely spin on its vertical axis by means of a bearing (Fig. 4) in order to prevent the apparition of torques at the tip. The physical characteristics of the beam and the tip mass are specified in Tables I and II. Tip mass includes the bearing mass.

The tip load of the bar is a disk floating over an air table which allows us to cancel the effects of gravity, and makes the friction of the movement almost inappreciable. On the other hand, the base of the bar is attached to the output axis of the motor which drives the system.

Fig. 3. Experimental platform

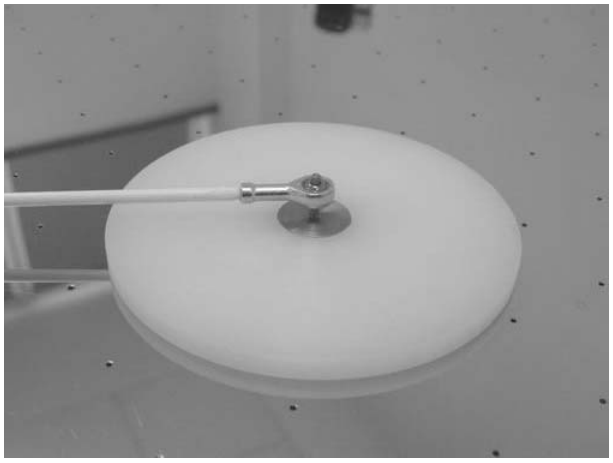

Fig. 4. Detail of tip joint

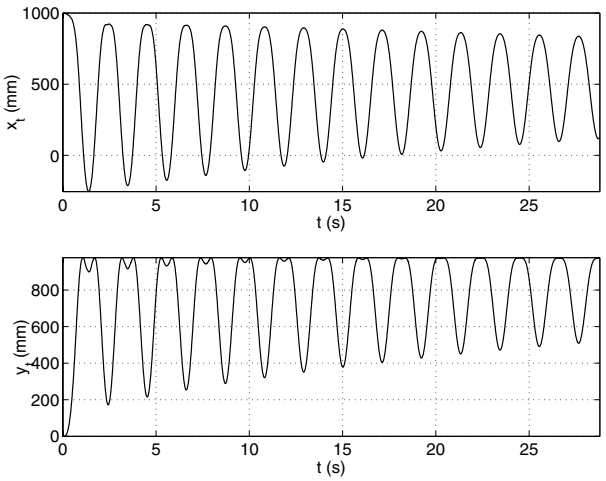

Fig. 5. Experimental cartesian coordinates of tip position

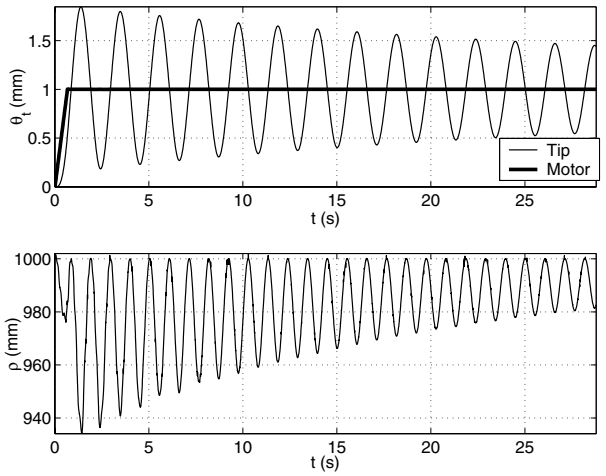

Fig. 6. Experimental polar coordinates of tip position

Our sensor system is integrated by an encoder embedded in the motor and a camera-based system for 3D position measurement. The first one allows us knowing the motor angle with a precision of $7{\cdot}10^{-5}$ rad. The second one consists of a set of three cameras that gives the tip position and the base position by means of a pair of spherical markers which reflect the infrared light. The precision of this system is 0.3 mm.

B. Experimental results

We have carried out several experiments of driving our lightweight fiberglass arm with the previously described setup. In particular we present in this communication the dynamic behavior produced by a motor motion of 1 rad at a speed of $\dot{\theta}_m = 1$ rad/sec. This maneuver produces very large deflections, and the arm behavior is clearly nonlinear.

Material	Mass (g)	Diameter (mm)	Height (mm)
Nylon	43.76	91.4	5.3

TABLE II

DATA OF THE TIP MASS

The experimental motion of the tip is shown in Fig. 5 (cartesian coordinates) and Fig. 6 (polar coordinates), where it has been supposed that $\theta_{t0} = 0$ rad, being θ_{t0} the initial tip angle, and therefore $y_{t0} = 0$ mm. Upper part of Fig. 6 also shows motor trajectory.

These figures evidence the nonlinearities of our model, as long as the maximum deflection reaches 0.85 radians ($48.7°$), and the radius variation is about 7 cm length, (7% of the total arm length), which is sensible enough to have to be taken into account.

C. Model fitting

Fitting process yields to the following parameters values.

- Linear model presented in equation (13)

$$\left.\begin{array}{l} \xi_l = 0.0458 \\ \omega^2 = 8.9671 \end{array}\right\} \tag{17}$$

- Non linear model of tip angle dynamics described by

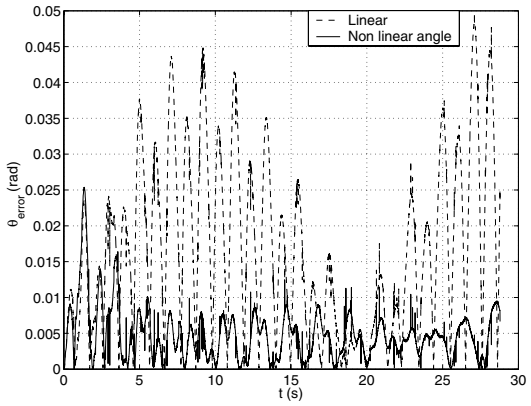

Fig. 7. Tip angle error between models and experiment

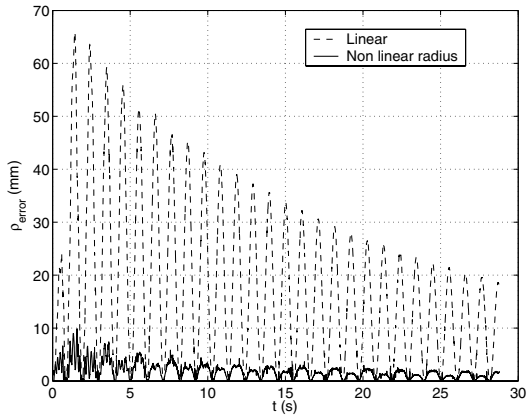

Fig. 8. Tip radius error between models and experiment

equation (15)

$$\left.\begin{array}{c}\xi_{nl} = 0.0458 \\ \alpha = 8.7907 \\ \beta = 0.5139\end{array}\right\} \tag{18}$$

- Non linear model for radius stated in equation (16)

$$\gamma = 0.4462 \tag{19}$$

The parameters of models (13), (15) and (16) have been fitted with the help of the technical computing program *MATLAB*™ by means of its least-square functions (Levenberg-Marquardt algorithm).

Fig. 7 shows the absolute fitting error between the angle of the tip and models (13) and (15) with their experimentally estimated parameters.

The nonlinear model clearly is more accurate than the linear one: at the beginning both models exhibit similar errors but the whole mean error is reduced from 0.0167 rad to 0.0048 rad.

Fig. 8 shows the absolute error in the radius of the tip position (distance to the origin). In the linear model this radius remains constant and equal to l, while in the non linear model it changes according to (16). This figure shows that the maximum error is reduced seven times: goes from 17.6 mm in the linear model to 1.8 mm using (16).

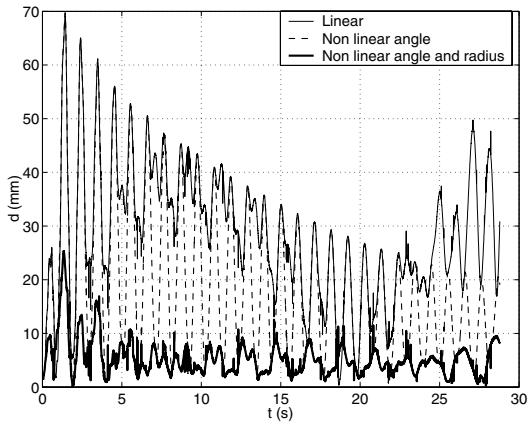

Fig. 9. Absolute position error between models and experiment

Finally, Fig. 9 displays the absolute tip position error (distance) between the experimental data and 1) the linear model, 2) the nonlinear spring model (15), and 3) the nonlinear spring model combined with (16).

Examining this figure we can notice some interesting results. Even though we achieve a moderate enhancement in the fitted model (15), and its mean error is lower than the linear model one, (19.2 to 28.3 mm), the major improvement of our model is attained with the inclusion of the radius nonlinearity model (16), which diminishes the peak error from 69.2 to 25.3 mm, and the mean error from 28.3 to 5.3 mm.

Figs. 10 and 11 show the responses of the different models in cartesian coordinates during the first 6 seconds of the registered motion. Figs. 12 and 13 show these responses at the end of the registered data. A difference in the vibration frequency between the experimental response and the one given by the linear model can be noticed in these last figures (the frequency of the real oscillation changes with time).

V. Conclusions

A simple nonlinear dynamic model has been proposed for single link very flexible and very lightweight arms made of a composite material. This model has been validated experimentally and exhibits the following features:

1) The nonlinear equations are of very simple form.
2) The equation that describes the tip angle dynamics is decoupled from radius variations.
3) A static relationship is proposed between the tip radius and the angular deflection of the tip $(\theta_t - \theta_m)$.
4) Friction of the disc on the air table and internal energy dissipation in the beam are adequately modeled by a linear term which depends on the tip velocity.
5) This model is quite accurate and captures adequately the significant dynamics of the arm: it has errors less than 20% of the errors of the linear model.
6) This model can be used to describe arms of any geometric dimensions, elasticity coefficient and tip mass, because of the normalized equation (9). Only the massless beam condition has to be preserved.

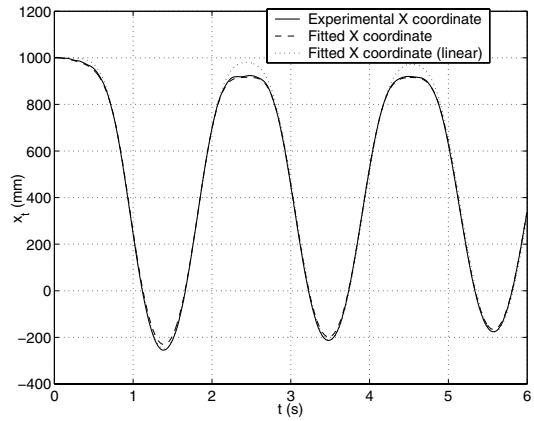

Fig. 10. Comparison between experiment and models. X coordinate (I)

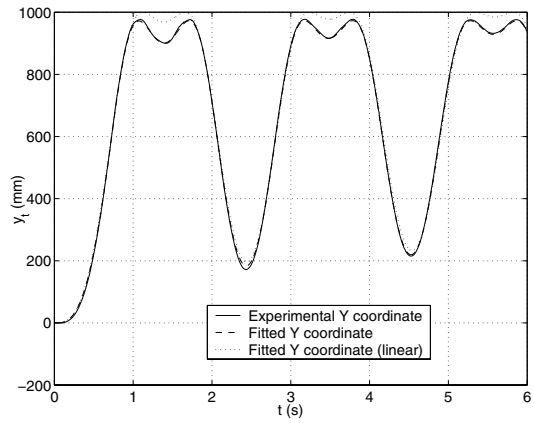

Fig. 11. Comparison between experiment and models. Y coordinate (I)

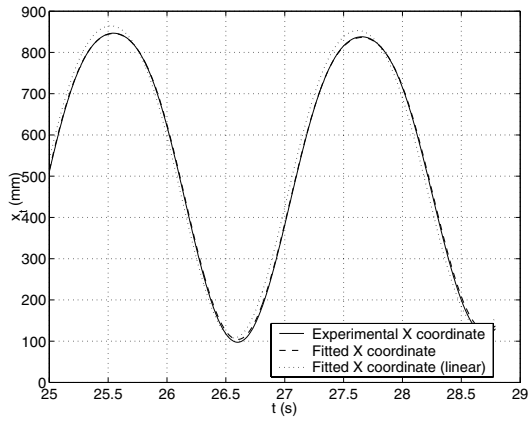

Fig. 12. Comparison between experiment and models. X coordinate (II)

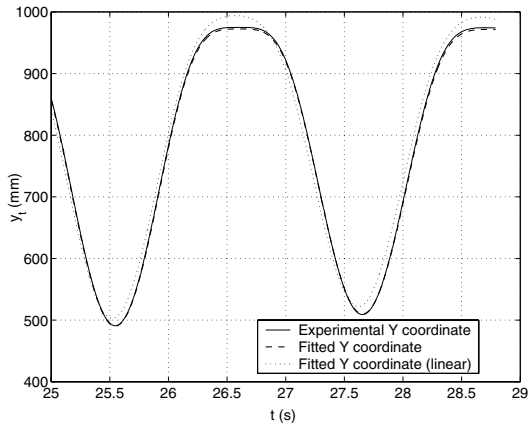

Fig. 13. Comparison between experiment and models. Y coordinate (II)

The proposed model is adequate for analysis and design of nonlinear closed loop control systems for tip positioning of this arm.

Finally we mention that this is the first step on a more extensive research where effects of non negligible inertia at the tip, and distributed mass through the arm will be considered.

REFERENCES

[1] M. Benosman and G. Le Vey, Control of Flexible Manipulators: A Survey, *Robotica*, vol. 22, pp. 533-545, (2004).

[2] W. O'Connor and D. Lang, Position Control of Flexible Robot Arms Using Mechanical Waves, *ASME Journal of Dynamic Systems, Measurement, and Control*, vol. 120, pp. 334-339, (1998).

[3] V. Feliu, K.S. Rattan and H.B. Brown, *Modelling and Control of Single-Link Flexible Arms with Lumped Masses*, ASME Journal of Dynamic Systems, Measurement, and Control, vol. 114, pp. 59-69, (March 1992).

[4] O. Morgul, On Boundary Control of Single Link Flexible Robot Arms, *IFAC Triennal World Congress*, San Francisco (USA), pp. 127-132, (1996).

[5] F. Boyer and R. Coiffet, Symbolic Modelling of a Flexible Manipulator via Assembling of its generalized Newton-Euler Model, *Mechanism and Machine Theory*, vol. 31, pp. 45-56, (1996).

[6] W.J. Book, Recursive lagrangian dynamics of flexible manipulator arms, *International Journal of Robotic Research*, vol. 3, no. 3, pp. 87-101, (1984).

[7] E. Bayo, A Finite-Element Approach to Control the End-Point Motion of a Single Link Flexible Robot, *Journal of Robotics Systems*, vol. 4, no. 1, pp. 63-75 (1987).

[8] E. Bayo, R. Papadopoulos, J. Stubbe and M. Serna, Inverse Dynamics and Kinematics of Multi-Link Elastic Robots: An Iterative Frequency Domain Approach, *Int. Journal of Robotics Research*, vol. 8, no. 6, pp. 49-62, (Dec. 1989).

[9] C.Y. Wang, Large Deflections of an Inclined Cantilever with an End Load, *International Journal of Non-Linear Mechanics*, vol. 16, no. 2, pp. 155-164, (1981).

[10] T. Belendez, C. Neipp and A. Belendez, Large and Small Deflections of a Cantilever Beam, *European Journal of Physics*, vol. 23, pp. 371-379, (2002).

[11] K. Lee, Large Deflections of Cantilever Beams of Non-Linear Elastic Material Under a Combined Loading, *Int. J. Non-Linear Mechanics*, vol. 37, pp. 439-443, (2002).

[12] K. Lee, J.F. Wilson and S.J. Oh, Elastica of Cantilevered Beams with Variable Cross Section, *Int. J. Non-Linear Mechanics*, vol. 28, no. 5, pp. 579-589, (1993).

[13] M. Gu and J-C. Piedboeuf, A Flexible-Arm as Manipulator Position and Force Detection Unit, *Control Engineering Practice*, vol. 11, pp. 1433-1448, (2003).

[14] I. Sharf, Geometrically Non-Linear Beam Element for Dynamics of Multibody Systems, *Int. J. for Numerical Methods in Engineering*, vol. 39, pp. 763-783, (1996).

[15] F. Boyer, N. Glandais and W. Khalil, Flexible Multibody Dynamics Based on a Non-Linear Euler-Bernouilli Kinematics, *Int. J. for Numerical Methods in Engineering*, vol. 54, pp. 27-59, (2002)

[16] S.P. Timoshenko and J.M. Gere, *Mechanics of materials*, Grupo Editorial Iberoamericana, 1986

[17] L.D. Landau and E.M. Lifshitz, *Theory of Elasticity*, Editorial Reverté S.A, 1969